Available online at www.academicpaper.org

Academic @ Paper

ISSN 2146-9067

International Journal of Automotive Engineering and Technologies

Vol. 4, Issue 4, pp. 162 –171, 2015

International Journal of Automotive Engineering and Technologies

http://www.academicpaper.org/index.php/IJAET

Original Research Article

Rollover Prevention System for the Commercial Truck Based on Controlling the Steering Angle

Emre Sert[1*], Sertac Dileroglu[1], Buket Kaya[2]

[1]Resarch and Development Department, Anadolu Isuzu Automotive Industry and Trade, Inc, Kocaeli, 41435, Turkey
[2]Marmara University, İstanbul, 34100, Turkey

Received 09 July 2015 Accepted 04December 2015

Abstract

Studies have shown that road accidents usually result in rollover. Therefore, the rollover dynamic is one of the most significant vehicle dynamic issues. The main objective of this study is to increase the safety margin of the commercial vehicle based on controlling the steering angle. The two-wheel vehicle model have been performed in order to obtain yaw rate and body lateral slip angle. Then, rollover model have been performed in order to obtain roll angle and roll rate of the vehicle during maneuvers. After Linear quadratic regulator and pole placement control system were used as the controller, uncontrolled system result was compared with the results of the two different controlled systems. The results indicate that pole placement controller gives better results than LQR in specific case.

Keywords: Rollover Dynamics, Commercial Vehicle, Controller Applications, Linear Quadratic Regulator, Vehicle Dynamics

Nomenclature

δ	: Steering Angle (rad)
β	: Sideslip angle at vehicle CG (rad)
$\alpha_ö$	: Sideslip angles at the front tire (rad)
α_a	: Sideslip angles at the rear tire (rad)
$C_ö$	: Cornering stiffness of the front Wheel (N/rad)
C_a	: Cornering stiffness of the rear Wheel (N/rad)
ϕ	: RollAngle (rad)
$\dot{\phi}$	: Roll Rate (rad/sn)
$\dot{\psi}$	: Yaw Rate (rad/sn)
α_y	: Lateral Acceleration (m/sn^2)
m	: Vehicle Mass (kg)
$\ddot{\psi}$	: Yaw acceleration (rad/sn^2)

Mz	: Angular Momentum around z-axis(N mm)
Fy	: Lateral Force (N)
l_v	: Longitudinal CG position measured the front axle (m)
l_h	: Longitudinal CG position measured the rear axle (m)
T	: Track Width (m)
k	: Suspension Spring Stiffness (kg m^2/sn^2)
c	: Suspension Damping Coefficient (kg m^2/sn)
h	: CG Height Measured over the Ground (m)
V_x	: Longitudinal Speed (m/sn)
V_y	: Lateral Speed (m/sn)
J_{zz}	: Yaw moment of inertia of the chassis measured at the CG (kg m^2)

*Corresponding Author:
E-mail: emre.sert@isuzu.com.tr

1. Introduction

Commercial vehicles occur stability problems if the drivers have to make a quick maneuver in order not to impinge on an unexpected obstacle. Studies have shown that road accidents usually result in rollover. [1]. Therefore, rollover related accidents became the new target of the studies in the field of vehicle dynamics research.

In Germany, 5% of vehicle accidents have resulted in rollover [2]. The studies conducted in the UK show that 13% of vehicle accidents were caused by rollover [2]. According to research conducted in the U.S, in 2001, the rollover accidents been accounted in 21% of total accidents [2]. The ratios of the accidents occurred in Turkey are shown as Table 1.

Table 1. The Accident Datas Occurred in Turkey [1]

Kazanın oluş şekli Nature of accidents	Kaza - Accidents			Sürücü - Driver		Yolcu - Passenger		Yaya - Pedestrian	
	A	B	C	D	E	D	E	D	E
					Toplam - Total				
Toplam - Total	**110 803**	**2 032**	**108 771**	**975**	**78 739**	**1 134**	**94 945**	**473**	**20 465**
Karşılıklı çarpışma - Crashed from reciprocal	6 539	236	6 303	186	6 711	227	6 942	5	54
Arkadan çarpma - Crashed from behind	12 033	219	11 814	122	9 025	148	13 725	4	265
Yandan çarpma - Crashed from side	36 561	282	36 279	190	31 598	165	33 100	7	664
Duran araca çarpma - Collision with standing vehicle	3 011	48	2 963	24	2 201	25	2 107	16	470
Sabit cisme çarpma - Collision with stationary object	11 638	213	11 425	121	9 016	138	10 819	8	385
Yayaya çarpma - Hitting pedestrian	17 917	423	17 494	6	1 233	2	608	428	18 375
Hayvana çarpma - Hitting animal	399	4	395	3	297	1	404	-	30
Devrilme - Overturn	7 858	177	7 681	96	6 786	127	8 370	3	53
Yoldan çıkma - Running off road	14 351	423	13 928	224	11 746	297	18 434	2	141
Araçtan düşen insan - Persons drapped from the vehicle	448	6	442	3	99	3	395	-	22
Araçtan düşen cisim - Supplies drapped from the vehicle	48	1	47	-	27	1	41	-	6

The main group of vehicles were more prone to rollover accidents are trucks and heavy vehicles [3]. Rollover dynamics can be neglected for cars but it cannot be neglected for especially heavily loaded trucks during maneuver. Therefore, in this study, a virtual model of the commercial truck (e.g. a heavy vehicle) is used for evaluating the stability.

The purpose of this paper is improving the response handling and preventing rollover based on controlling the steering angle. Mathematical models of the yaw and roll dynamics have been formed. Then, the full vehicle model is completed by combining sub-systems such as yaw, roll and steering models using Matlab/Simulink programme.

The first step in this project is to measure the initial parameters using real Fishhook test. Matlab model is confirmed based on the measured parameter. Therefore, initial parameters of the model are the same as the actual vehicle.

Load transfer ratio effects the handling balance of the vehicle and it causes rollover. Therefore, dynamic load transfer ratio (DLTR) was used as the system output. Calculations were completed to investigate these loads and their effects. This tutorial have guided to understand how controller types affect the DLTR value. After the determination of the boundary conditions, the controller design has been performed in order to increase the safety margin. DLTR has been tuned using the well-known the two different control theories, which are pole placement method and LQR. Two different controller were considered here and the performance of each controller was compared with the other one. The signals of the yaw rate, roll angle, roll rate and body lateral slip angle have been selected as state variables of the simulation model. Moreover, the steering angle has been selected as input of the simulation model. Amongst the standard testing maneuvers, the Fishhook maneuver was the most repeatable of all rollover resistance maneuvers performed in the study [4, 5].

Cornering represents a dangerous situation when a vehicle attempts to turn a corner quickly. Therefore, controller design was performed using Fishhook maneuver. In the simulations without the controllers, a dynamic load transfer ratio was calculated as 1.074. However, it is observed that DLTR value can be decreased as 0.85 if the controller was included in the loop.

2. Vehicle Mathematic Model

Isuzu commercial truck model have been chosen as the improvement vehicle. All vehicle parameters exist within the vehicle dynamics library of the Isuzu. The geometric dimension of the truck is shown as Figure 1.

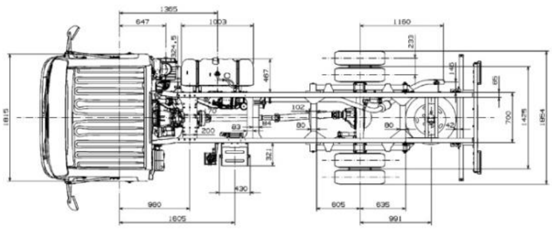

Figure 1 Geometric Dimensions of the Truck

Gross vehicle weight (GVW) is the condition that has more tendency for roll over. Therefore, the vehicle have been handled as GVW. Vehicle parameters are shown in the Table 2.

Table 2. Technical specification of the Midi Bus

Vehicle Parameters	Measurements
Wheelbase	3365 (mm)
Length	6123 (mm)
Width	2040 (mm)
Height	2275 (mm)
Front track width	1680 (mm)
Rear Track width	1650 (mm)
Center of Gravity Height	1450 (mm)
Gross Weight Vehicle	8000 (kg)

Combined with steering angle input, a two-wheel model was used as reference model in determining vehicle yaw stability status. Firstly, a two-wheel vehicle model have been performed in order to obtain yaw rate and body lateral slip angle during maneuvers. The two-wheel vehicle model is shown in Figure 2.

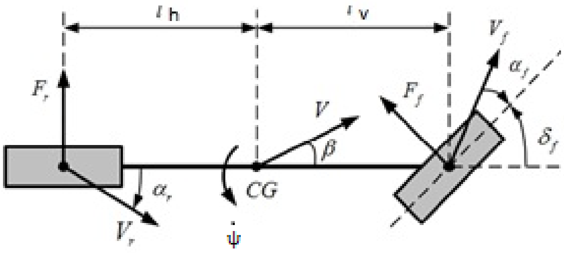

Figure 2 Two-Wheel Model of the Vehicle

Figure 2 represents sideslip angle (β) and yaw rate ($\dot{\psi}$) measured at the CG. The lateral tire forces F_f and F_r are expressed by Equation 1.

$$\sum F_y = ma_y = F_f \cos(\delta) + F_r \quad (1)$$

Angular Momentum around the axis of rotation z axis (M_z) are described by Equation 2 [4].

$$\sum M_z = \ddot{\psi} J_{zz} = l_v F_f \cos(\delta) - l_h F_r \quad (2)$$

Where $\ddot{\psi}$ is the yaw acceleration, J_{zz} is the yaw moment of inertia of the chassis measured at the CG. l_v is the Longitudinal CG position measured the front axle, l_h is the Longitudinal CG position measured the rear axle and δ is the steering angle.

Steering angle (δ) is small. So that, cos(δ) =1and sin (δ) =0areassumed. Arranging equations 1 and 2, the following set of equations can be obtained.

$$\sum F_y = ma_y = F_f + F_r \quad (3)$$

$$\sum M_z = \ddot{\psi} J_{zz} = l_v F_f - l_h F_r \quad (4)$$

Also notice that since we assume small angles and constant longitudinal velocity, sideslip angle (β) satisfies the following

$$\beta = \frac{v_y}{v_x} \text{and} \dot{\beta} = \frac{\dot{v_y}}{v_x} \quad (5)$$

According to the linear tire model, front wheel side slip angle (α_o) is expressed by Equation 6.

$$\alpha_ö = \tan^{-1}\left(\frac{v_{öy}}{v_{öx}}\right) - \delta = \delta - \beta - \frac{l_v}{v_x}\dot{\psi} \quad (6)$$

Where V_{ox} is the longitudinal speed of the front wheel, V_{oy} is the lateral speed of the front wheel. Rear wheel side slip angle (α_a) is expressed by Equation 7.

$$\alpha_a = \tan^{-1}\left(\frac{v_{ya}}{v_{xa}}\right) = -\beta + \frac{l_h}{v_x}\dot{\psi} \quad (7)$$

Where V_{ax} is the longitudinal speed of the rear wheel, V_{ay} is the lateral speed of the rear wheel.

Nominal cornering stiffness of the front wheels is illustrated as C_o and nominal cornering stiffness of the rear wheels is illustrated as C_a. Lateral tire forces are approximated as linear functions of cornering stiffness and the wheel slip angle. They are expressed by Equation 8 and 9.

$$F_f = C_ö \text{ x } \alpha_ö = C_ö\left(\delta - \frac{v_y + l_v \psi}{v_x}\right) \quad (8)$$

$$F_r = C_a \text{ x } \alpha_a = C_a\left(\frac{v_y - l_h \psi}{v_x}\right) \quad (9)$$

Where V_y is the lateral speed of the vehicle and V_x is the longitudinal speed of the vehicle. Finally, equation 10 is obtained with arranging equation 4.

$$\ddot{\psi} J_{zz} = C_ö\left(\delta - \frac{v_y + l_v \psi}{v_x}\right) + C_a\left(\frac{v_y - l_h \psi}{v_x}\right) \quad (10)$$

Rollover model have been performed in order to obtain roll angle and roll rate of the vehicle during maneuvers. The 3-dof model considering roll movement is a simple yet most commonly used vehicle model in rollover prevention as in Figure 3. This model is developed from the Euler-Lagrange method. Figure 3 also illustrates the key factors in the tendency of heavy vehicles to roll over. It is also described as linear functions of track width (T) and CG height (h) as well as the parameters of the suspension system k and c. Lateral acceleration acting on the CG creates a roll moment about the suspension roll center.

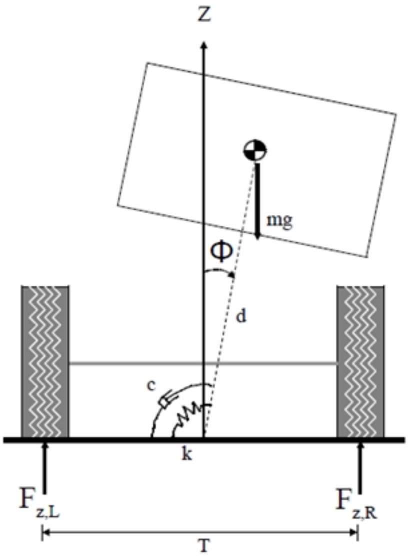

Figure 3 Rollover Model of the Vehicle [6]

This model is developed from the Euler-Lagrange method. Figure 3 also illustrates the key factors in the tendency of heavy vehicles to roll over. It is also described as linear functions of track width (T) and CG height (d) as well as the parameters of the suspension system k and c. Lateral acceleration acting on the CG creates a roll moment about the suspension roll centre.

Lateral forces are expressed by Equation 11.

$$\sum F_y = ma_y - mh\ddot{\varnothing}\cos(\varnothing) - mh\dot{\varnothing}^2\sin(\varnothing) \quad (11)$$

Where m is the vehicle mass, a_y is the lateral acceleration, h is the CG height measured over the round, Ø is the roll angle. Roll angle of the unsprung mass Ø is small. So that,

$\cos(\varnothing)=1$, $\sin(\varnothing)=\varnothing$, $mh\dot{\varnothing}^2=0$are assumed.

Arranging equations 8 and 9, the following set of equations can be obtained.

$$m\dot{v}_y + m\dot{\psi}v_x - mh\ddot{\varnothing} = C_{\ddot{o}}\left(\delta - \frac{v_y + l_v\psi}{v_x}\right) + C_a\left(\frac{v_y - l_h\psi}{v_x}\right) \quad (12)$$

Using the parallel axis theorem, the moment of inertia of the vehicle (J_{ag}) about the assumed roll axis can be computed by Equation 13.

$J_{ag}=J_{xx}+mh^2$ So that,

$$mha_y + \left(J_{xx}+mh^2\right)\ddot{\varnothing} = -c\dot{\varnothing} - k\varnothing + mgh\sin(\varnothing) \quad (13)$$

Lateral acceleration is expressed by the following equation.

$$a_y = (\dot{v}_y + \dot{\psi}v_x)$$

Equation 14 is obtained with arranging the lateral acceleration.

$$\sin(\varnothing) = mh\dot{v}_y + \left(J_{xx}+mh^2\right)\ddot{\varnothing}$$
$$= -mh\dot{\psi}v_x - c\dot{\varnothing} - k\varnothing + mgh\varnothing \quad (14)$$

Arranging equations 5,12 and 14, the following set of equations can be obtained.

$$m\dot{\beta}v_x - mh\ddot{\varnothing} \doteq$$
$$= -m\psi v_x - (C_{\ddot{o}}+C_a)\beta + \left(C_a l_h - C_{\ddot{o}} l_v\right)\frac{\psi}{v_x} + \delta C_{\ddot{o}} \quad (15)$$

$$\ddot{\psi}J_{zz} =$$
$$= \left(C_a l_h - C_{\ddot{o}} l_v\right)\beta - \left(C_{\ddot{o}} l_v^{\,2} + C_a l_h^{\,2}\right)\frac{\dot{\psi}}{v_x} + \delta C_{\ddot{o}} l_v \quad (16)$$

$$-mh\dot{\beta}v_x + \left(J_{xx}+mh^2\right)\ddot{\varnothing} =$$
$$= mh\psi v_x - c\dot{\varnothing} - k\varnothing + mgh \quad (17)$$

Equations 15, 16 and 17 were arranged because roll angle, roll rate, yaw rate and body lateral slip angle must be in the left half plane.

3. Dynamic Load Transfer Ratio

Dynamic load transfer ratio (DLTR) is defined by the relationship between wheel loads and center gravity height of the vehicle [6]. Equation 18 represents dynamic load transfer ratio.

$$DLTR = \frac{\text{Right wheel load-Left wheel load}}{\text{Total wheel load}} \quad (18)$$

We can write a force balance for the unsprung mass about the assumed roll axis in terms of the suspension forces as shown Equation 19.

$$DLTR = \frac{2}{m*g*T}(k\,\varnothing + c\dot{\varnothing}) \quad (19)$$

Dynamic load transfer ratio was selected as the system output. It is evident that this parameter varies in the interval [−1, 1] and during straight driving for a perfectly symmetric car it is 0.The extremum is reached in the case of a wheel lift-off of one side of the vehicle, in which case it becomes 1 or −1.Therefore, a direct measurement of this parameters can be used as a rollover warning.

4. State Space Equations

The corresponding linearized equations will be written in the state space form, the following set of equations can be obtained.

$\dot{x}=Ax+Bu$

$$y = [C][x]$$

where$x = [\beta \quad \dot{\psi}\dot{\varnothing} \quad \varnothing]^T$

Roll angle, roll rate, yaw rate and body lateral slip angle are chosen as state variables. All state variables of the initial conditions were measured using real vehicle test. The steering angle is chosen as input parameter of the system as written below.

$B_{\delta}=[\delta]$

We can define the auxiliary variables as written below.

$\sigma = C_a + C_{ö}$

$\rho = l_h C_a - l_v C_{ö}$

$Ꝃ = l_h{}^2 C_a + l_v{}^2 C_{ö}$

State space form can be obtained when using previous equation of 15, 16 and 17.

$$\begin{bmatrix} \dot{\beta} \\ \ddot{\psi} \\ \ddot{ø} \\ \dot{ø} \end{bmatrix} = \begin{bmatrix} -\frac{\sigma}{mv_x}\frac{J_{eq}}{J_{xx}} & \frac{\rho}{mv_x}\frac{J_{eq}}{J_{xx}} - v_x & -\frac{hc}{J_{xx}} & \frac{h(mgh-k)}{J_{xx}} \\ \frac{\rho}{J_{zz}v_x} & -\frac{Ꝃ}{J_{zz}v_x} & 0 & 0 \\ -\frac{h\sigma}{J_{xx}v_x} & \frac{h\rho}{J_{xx}v_x} & -\frac{c}{J_{xx}} & \frac{mgh-k}{J_{xx}} \\ 0 & 0 & 1 & 0 \end{bmatrix} \begin{bmatrix} \beta \\ \dot{\psi} \\ \dot{ø} \\ ø \end{bmatrix} + \begin{bmatrix} \frac{C_{ö}}{m}\frac{J_{eq}}{J_{xx}} \\ \frac{l_v C_{ö}}{J_{zz}} \\ \frac{hC_{ö}}{J_{xx}} \\ 0 \end{bmatrix} [\delta]$$

Where(δ) is the driver steering command from the actuator.

Output parameter of the system is written as Equation 20.

$$y = \begin{bmatrix} 0 & 0 & \frac{2c}{mgT} & \frac{2k}{mgT} \end{bmatrix} \begin{bmatrix} \beta \\ \dot{\psi} \\ \dot{ø} \\ ø \end{bmatrix} \qquad (20)$$

The vehicle is driven in a straight line. Then steering angle reaches 250 degree within three second with vehicles at a constant speed of v_x = 20m/s. The wheel is held at this angle for three seconds. Then it is turned back to zero degrees at a steady rate during the following three seconds. The Steering angle is shown in Figure 4.

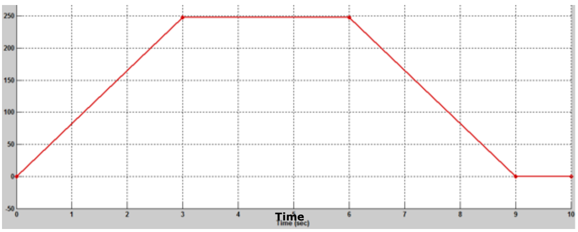

Fig. 4The Steering Angle When Fishhook Maneuver

DLTR exceeded the value of 1.074 shown in Figure 5 during the maneuver. Therefore, it was observed that the vehicle will be rollover. The maximum value of the DLTR will be compared with the results of the controller response (closed loop system).

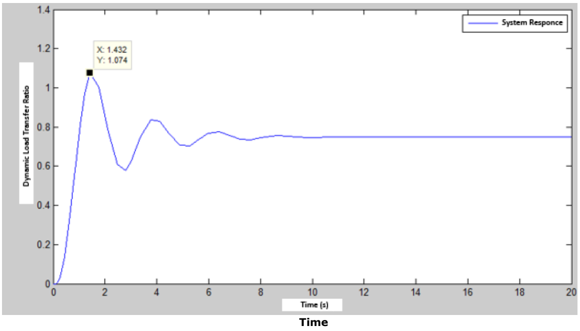

Fig. 5 Open System Response of the DLTR.

5. Controller Design

In this research, controllers will be designed for the vehicle around a nominal straight line trajectory. Therefore the state space representation of the linearized tracking error dynamics, as described in previous section, will be used.

The active steering control based on linear quadratic regulator and pole placement control improves the rollover significantly under the disturbance torque.

Numeric values are created by inserting parameters of the vehicle into the state-space equation. Equation 21 represents state-space equation of the rollover dynamics.

$$\begin{bmatrix} \dot{\beta} \\ \ddot{\psi} \\ \ddot{ø} \\ \dot{ø} \end{bmatrix} = \begin{bmatrix} -5.89 & -18.31 & -2 & -15.70 \\ 0.59 & -3.84 & 0 & 0 \\ -2.47 & 1.64 & -1.53 & -12.07 \\ & 001 & 0 & \end{bmatrix} \begin{bmatrix} \beta \\ \dot{\psi} \\ \dot{ø} \\ ø \end{bmatrix} + \begin{bmatrix} 41.66 \\ 14.00 \\ 17.50 \\ 0 \end{bmatrix} [\delta]$$

$$y = \begin{bmatrix} 0 & 0 & -0.30 & -4.25 \end{bmatrix} \begin{bmatrix} \beta \\ \dot{\psi} \\ \dot{ø} \\ ø \end{bmatrix} \quad (21)$$

Time-dependent graph of the roll angle (x1), roll rate (x2), yaw rate (x3) and body lateral slip angle (x4) are shown in Figure 6.

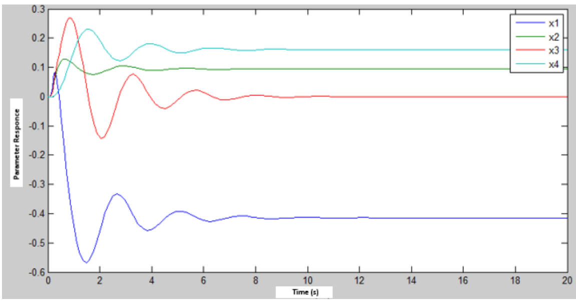

Fig. 6 Responses of Parameters

5.1 Controllability

It is mandatory to investigate how the system can be controlled before starting the control design. Uncontrollable systems have certain modes unaffected by the law of control. The mathematical test gives information about states of the system (A, B) which is the rank of the controllability matrix. The controllability matrix has been found as Equation 22.

$A_{A,b}$=[B ABA^{2}B A^{3}B]then,

$$A_{A,b}=\begin{bmatrix} 42 & -537 & 3632 & -18353 \\ 14 & -29 & -21 & 2975 \\ 18 & -107 & 1235 & -9941 \\ 0 & 18 & -107 & 1235 \end{bmatrix} \quad (22)$$

The system (A, B) is controllable if the rank of A matrix is equal to the number of the states. It is possible to indicate the controllability of a system with the placed actuators (inputs) on the system. Rank of the system is calculated as four. Therefore, the system can be controlled under these assumptions.

The controllability of the system output have been obtained as the following equation.

$C_{0A,b}$=[-5.4 -41.3 73.4 -2176.8]

Rank of the system output is calculated as one. Therefore, the system output is controllable.

5.2 Controller Companion Form

State space equations must be transformed to controller companion form in order to design controller matrices. Equation 23 represents controller companion form.

$$A_C=\begin{bmatrix} 0 & 10 & 1 \\ 0 & 01 & 0 \\ 0 & 00 & 1 \\ -271.64 & -113.31 & -55.67-11.27 \end{bmatrix}$$

$$B_C=\begin{bmatrix} 0 \\ 0 \\ 0 \\ 1 \end{bmatrix} \text{ and}$$

$$C_C=\begin{bmatrix} -4459.3 & -793.4 & -116.1 & -2 \end{bmatrix} \quad (23)$$

5.3 Pole Placement Method

The purpose of the control law is to assign a set of desired (control) pole locations of the closed loop system which corresponds with a satisfactory dynamic behavior.

Necessary parameters should be determined based on the expected performance of the system. Rollover is a condition that occurs suddenly [7]. Therefore, controller response should become more quickly and it should not exceed a maximum value.

Maximum exceed and damping ratio were selected as desired performance characteristics obtained as the following equation.

- Maximum exceed is %5

$$\sigma=e^{-\frac{\xi\pi}{\sqrt{1-\xi^2}}} \quad (24)$$

Where σ is the damping ratio

Settlement time is based on the responses of the state variables in open loop system.

- Settlement time for the system is 15 second

$$t_s=\frac{\pi}{w_n\sqrt{1-\xi^2}} \quad (25)$$

Where w_n is the natural frequency

The system must be 4-pole so it has four degrees of freedom. Damping ratio and natural frequency are dominant poles determined the behavior of the system. w_n, ξ and two poles in second order are described as Equation 26:

$$s^2+2\xi w_n s+w_n^2 \quad (26)$$

The locations of the desired control poles were arbitrary chosen and two poles of the system were computed according to the damping ratio as shared below.

$\lambda_{1,2}$= -0,5991∓j0,6283

Other two poles chosen for controller must be placed on the left plane of the open loop system poles. Therefore, two roots were selected as $\lambda_{3,4}$ =-5

Controller system function is computed as Equation 27.

$$s^4+11.198s^3+37.736s^2+37.494s+18.844 \quad (27)$$

System matrix can be computed as following equation

$$A_d=A_C-b_C k_C$$

It is obtained as Equation 28.

$$A_d=\begin{bmatrix} 0 & 10 & 0 \\ 0 & 01 & 0 \\ 0 & 00 & 1 \\ 18.8440 & 37.4949 & 37.7367 & 11.1983 \end{bmatrix} \quad (28)$$

The controller coefficient is computed as Equation 29,

k_c^T=[-252.8046-75.8157-17.93770.0739] (29)

LQR model was created as shown in Figure 7

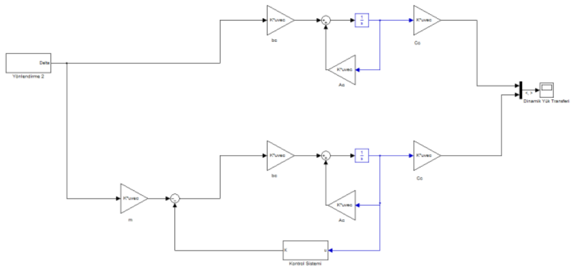

Fig. 7Simulink model of the Pole Placement Controller

The maximum value of the DLTR under uncontrolled system is compared with the result of the controller response as shown in Figure 8.

Blue line represents the result of the uncontrolled system and the green line represents the result of the controlled system. It is observed that the controller reduces DLTR value when compared to the result of the uncontrolled system.

Dynamic Load Transfer Ratio is calculated as 0.7802 under pole placement controller design. Therefore, increment of the safety margin in percentage is calculated as % 27.355. The possibility of rollover of the vehicle is prevented and the vehicle remains safe region under the specified test conditions.

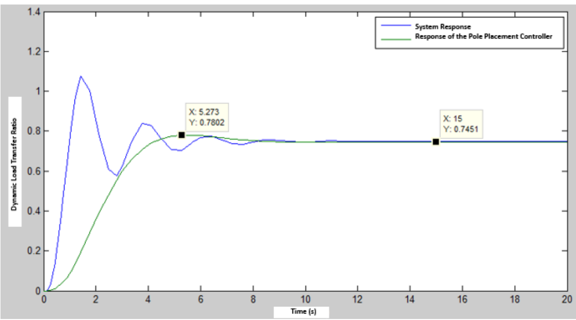

Fig. 8 Comparison of System Response and Controller Response

5.4 Linear Quadratic Regulator

In this section, LQR design with control coupled output regulation is proposed and it is applied to a vehicle dynamics problem. Popular method for control design of linear dynamic systems is called as the LQR method. Recalling the performance index in LQR design is denoted by J. Furthermore, the purpose of the study is to minimize the cost function which can be described in Equation 30:

$$J=\frac{1}{2}\int_0^{\infty}(\underline{x}^T(t)*Q*\underline{x}(t)+\underline{u}^T(t)*R*\underline{u}(t))dt \quad (30)$$

P (t) is constant, so $\dot{\underline{P}}(t)=0$is obtained.

Riccati equation can be described as Equation 31:

$$A(t)P(t)+A^T(t)P(t)-P(t)B(t)R(t)^{-1}\underline{B}^T(t)P(t)+Q(t) \quad (31)$$

Where R is the energy coefficient and Q is the performance matrix

Q and R that are design parameters represent performance outputs of the trajectory y and the control input u. The rule of the optimal control is described as Equation 32:

$$\underline{u}(t)=-R(t)\underline{B}^T(t)P\ (t) \quad (32)$$

Where P is the solution of the following Algebraic Riccati Equation (ARE).

The selection of R and Q determines how the system acts. Stabilization time of the system is changed with Q/R oscillation around the same regime. LQR model is created as shown in Figure 9. Red line represents system block of the LQR controller.

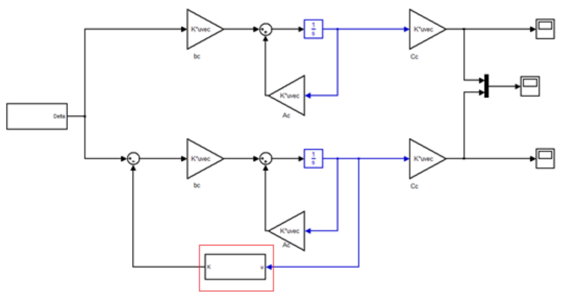

Fig. 9 Simulink model of the Quadratic Regulator Controller

Three different LQR controllers is designed in order to see the effects of Q and R. These values are founded by experimental trails. Experimental results are compared with the output in the time domain in order to provide a foundation for the remainder of the work.

5.4.1 Design 1

Energy coefficient (R) were assumed as equal to 1 and performance matrix (Q) was minor number matrix. First design is shown as Equation 33.

R=1 and Q= $\begin{bmatrix} 20000 \\ 04000 \\ 00700 \\ 00090 \end{bmatrix}$ (33)

The rule of the optimal control is expressed by the following equation.

$$\underline{u}(t) = -R(t)\underline{B}^{T}(t)P\,(t)$$

The controller coefficient is computed as Equation 34,

k_c^{T}=[0.0368 36.6433 17.6726 4.6151] (34)

The maximum value of the DLTR under uncontrolled system response is compared with the result of the first design response as shown in Figure 10.

Dynamic Load Transfer Ratio is calculated as 0.9282 under linear quadratic controller design. Whereas increment of the safety margin is calculated as % 13.575. The possibility of rollover of the vehicle is prevented and the vehicle remains safe region under the specified test conditions.

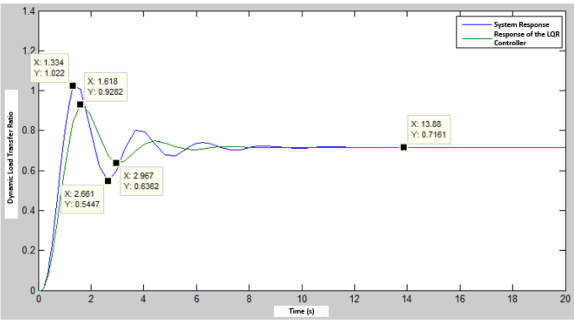

Fig. 10 Comparison of System Response and First Design Response

5.4.2 Design 2

Energy coefficient (R) were assumed as equal to 0.1 and performance matrix (Q) was minor number matrix. Second design is shown as Equation 35.

R=0.1 and Q= $\begin{bmatrix} 20000 \\ 04000 \\ 00700 \\ 00090 \end{bmatrix}$ (35)

The rule of the optimal control is expressed by the following equation.

$$\underline{u}(t) = -R(t) * \underline{B}^{T}(t) * P\,(t)$$

The controller coefficient is computed as Equation 36.

k_c^{T}=[0.3679 120.1191 75.7475 23.0579](36)

The maximum value of the DLTR under uncontrolled system response is compared to the result of the second design response as shown in Figure 11.

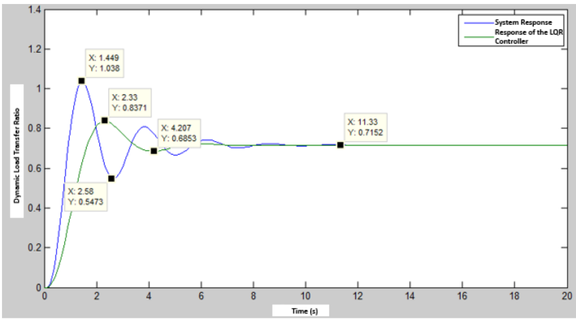

Fig. 11 Comparison of System Response and Second Design Response

As seen from the results in Figure 10, Dynamic Load Transfer Ratio is calculated as 0.8371 under linear quadratic controller design. Therefore, increment of the safety margin in percentage is calculated as % 22.057.

5.4.3 Design 3

We want to determine how interactions between factors affect the performance and significance. Energy coefficient (R) were assumed as equal to 1 and performance matrix (Q) was major number matrix. Third design is shown as Equation 37.

R=1 and Q= $\begin{bmatrix} 100 & 0 & 0 & 0 \\ 0 & 120 & 0 & 0 \\ 0 & 0 & 150 & 0 \\ 0 & 0 & 0 & 170 \end{bmatrix}$ (37)

The rule of the optimal control is expressed by the following equation.

$$\underline{u}(t) = -R(t)\underline{B}^{T}(t)P\,(t)$$

The controller coefficient is computed as Equation 38.

k_c^{T}=[0.1840 54.7046 28.0491 7.5204](38)

The maximum value of the DLTR under uncontrolled system response is compared with the result of the third design response as shown in Figure 12.

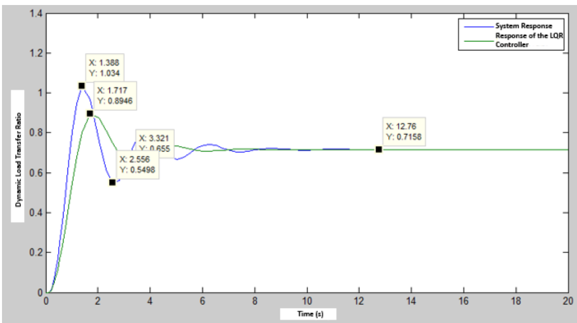

Fig. 12 Comparison of System Response and Third Design Response

As seen from the results in Figure 11, Dynamic Load Transfer Ratio is calculated as 0.8946 under linear quadratic controller design. Therefore, increment of the safety margin in percentage is calculated as % 16.703.
In the simulation results, the most effective controller is design 2 to regulate the output. Controller Design 3 cannot regulates the output as much as design 2. However, design 3 is more effective than the control design 1. To sum up, the design 2 is more effective than the controller design 3 and 1.

6. Conclusions

This paper presents an experimental approach of the rollover dynamics with the investigation on two different controller designs. Open loop system response and closed loop system controllers were compared.
Weight matrices of the Linear Quadratic Regulator were determined with experimental methods in the controller. When the energy coefficient (R) is decreasing, the LQR design based on the rollover performance index (Design 2) always yields a bigger safety margin compared with the design 1 and 3.However, the system response becomes slower. Similarly, when the performance matrix (Q) is increasing, the LQR design based on the rollover performance index (Design 3) always yields a bigger safety margin compared with the design 1.On the other hand, the system response becomes faster. Therefore, the parameters of R and Q must be determined according to the roots of the system. In this LQR study, controller is more effective for regulating the performance output if and only if the bigger performance matrix (Q) and smaller energy coefficient (R) are used.
Safety margin calculated using pole placement method is higher than calculated using LQR method. The results indicate that pole placement provides better results than LQR in specific case. The controller results are shown in Table 3.

Table 3. Controller Design Results

Controller Design		Increment of the Safety Margin in Percentage (%)
Linear Quadratic Regulator	Design 1	13.575
	Design 2	22.057
	Design 3	16.703
Pole Placement	Maximum exceed %5	27.355

System output turns out that there is a considerable difference in the performance of the controllers based on the proposed rollover performance index.
The analysis show that it is possible to maximize rollover threshold and increase vehicle stability by controlling the steering angle. Therefore, safety margin can increase by 27.355 % from their nominal value.

Acknowledgments

The authors would like to acknowledge the support of Anadolu Isuzu Automotive Industry and Trade, Research and Development Center.

7. References

[1] Traffic Accident Statistics, General Directorate of Public Security and Turkish Statistical Institute, 2011

[2] NHTSA, “Traffic Safety Facts 2001,” DOT HS 809 476, 2002.

[3] Chen, B.-C, Peng, Huei (2005). Rollover Warning for Articulated Heavy Vehicles Based on a Time-to-Rollover Metric. Transactions of the ASME, Vol. 127. Pp.406-414.

[4] S.Solmaz (2007). Topics in Automotive Rollover Prevention: Robust and Adaptive Switching Strategies for Estimation and Control.

[5] J. Ackermann and D. Odenthal, "Damping of vehicle roll dynamics by gain scheduled active steering," in Proc. European Control Conference, 1999.

[6] Sert, E., “Improving Rollover Dynamics Characteristics of the Bus using

Parameter Optimization and Controller Design," ITU, July 2014
[7] P. Ponticel (2003). Dynamic testing rollover on the way. Automot. Eng. Int., pp. 26–28.
[8] Parenteau, C., Thomas, P. and Lenard, J., "US and UK Field Rollover Characteristics," SAE 2001-01-0167, 2001.
[9] S.R., Ribeiro, M., E., Silveira, "Application of Finite Element Method in the Study of Variables that Influence the Stiffness of the Anti-Roll Bar and the Body Roll," SAE 2013-36-0643, 2013.
[10] Sert, E., Kizilca, S., D., Dileroglu, S., "Ride Comfort Sensitivity Analysis of Portal Axle Using Adams/Car," ISITES, 20 June 2014.
[11] Sert, E., Caliskan, T., Atasoy, H., "Static Rollover Characteristics of the Armored Vehicle," Otekon, May 2014.